Kim et al. World Allergy Organization Journal (2022) 15:100628
http://doi.org/10.1016/j.waojou.2022.100628

WORLD ALLERGY ORGANIZATION JOURNAL

Open Access

Phenotypic clusters on computed tomography reflects asthma heterogeneity and severity

Sujeong Kim, MD[a,†], Sanghun Choi, PhD[b,†], Taewoo Kim, BS[b], Kwang Nam Jin, MD, PhD[c], Sang-Heon Cho, MD, PhD[d,e], Chang Hyun Lee, MD, PhD[f,g,†*] and Hye-Ryun Kang, MD, PhD[d,e,†**]

ABSTRACT

Background: Asthma is a heterogeneous inflammatory airway disorder with various phenotypes. Quantitative computed tomography (QCT) methods can differentiate among lung diseases through accurate assessment of the location, extent, and severity of the disease. The purpose of this study was to identify asthma clusters using QCT metrics of airway and parenchymal structure, and to identify associations with visual analyses conducted by radiologists.

Methods: This prospective study used input from QCT-based metrics including hydraulic diameter (D_h), luminal wall thickness (WT), functional small airway disease (fSAD), and emphysematous lung (Emph) to perform a cluster analysis and made comparisons with the visual grouping analysis conducted by radiologists based on site of airway involvement and remodeling evaluated.

Results: A total of 61 asthmatics of varying severities were grouped into 4 clusters. From C1 to C4, more severe lung function deterioration, higher fixed obstruction rate, and more frequent asthma exacerbations were observed in the 5-year follow-up period. C1 presented non-severe asthma with increased WT, D_h of proximal airways, and fSAD. C2 was mixed with non-severe and severe asthmatics, and showed bronchodilator responses limited to the proximal airways. C3 and C4 included severe asthmatics that showed a reduced D_h of the proximal airway and diminished bronchodilator responses. While C3 was characterized by severe allergic asthma without fSAD, C4 included ex-smokers with high fSAD% and Emph%. These clusters correlated well with the grouping done by radiologists and clinical outcomes.

Conclusions: Four QCT imaging-based clusters with distinct structural and functional changes in proximal and small airways can stratify heterogeneous asthmatics and can be a complementary tool to predict clinical outcomes.

Keywords: Asthma, Phenotype, Tomography, X-ray computed, Airway remodeling

[a]Division of Allergy and Clinical Immunology, Department of Internal Medicine, School of Medicine, Kyungpook National University, Daegu, South Korea
*Corresponding author. Seoul National University College of Medicine, 101 Daehak-ro, Jongno-Gu, Seoul 110-744, South Korea. E-mail: changhyun.lee@snu.ac.kr
**Corresponding author. Seoul National University College of Medicine, 101 Daehak-ro, Jongno-Gu, Seoul 110-744, South Korea, Email: helenmed@snu.ac.kr
[†] These authors contributed equally to this article.
Full list of author information is available at the end of the article

http://doi.org/10.1016/j.waojou.2022.100628
Received 20 August 2021; Received in revised from 3 December 2021; Accepted 12 January 2022
Online publication date 5 February 2022

INTRODUCTION

The emphasis on the recognition of heterogeneity in asthma phenotypes has increased with the growing interest in personalized treatment. Clustering analysis is often performed in asthma to identify asthma phenotypes with distinct disease processes and prognoses. Various histological abnormalities have often been observed in the asthmatic airway, including epithelial goblet cell hyperplasia, increased smooth muscle mass, bronchial wall thickening, subepithelial fibrosis, and angiogenesis.[1–3] Airway remodeling, an important component of asthma pathophysiology, is characterized by structural changes that occur in lungs and airways due to chronic airway inflammation.[4–6] Most studies investigating clustering analyses have focused on findings primarily obtained from endobronchial biopsies of asthmatics. These studies are limited in that bronchoscopic evaluation is an invasive procedure that may not be readily available, and distal airway evaluation using bronchoscopy is oftentimes difficult.

Computed tomography (CT) scanning is a non-invasive and highly reproducible tool for the objective assessment of airway remodeling in asthmatics. Previous studies have shown that CT can identify diverse structural changes such as bronchial wall thickening, bronchial luminal dilation or narrowing, mosaic lung attenuation, and decreased lung attenuation on expiratory CT images.[7–11] These features of airway modeling observed in CT images also show strong correlations with pathological and functional examinations.[12,13]

Airway remodeling was more frequently observed in CT images of patients with severe asthma than in those with mild asthma. Although many attempts have been made to extend the current knowledge on severe asthma through recently advanced imaging technique such as quantitative CT (QCT) imaging,[10,14,15] little is known about whether different airway remodeling patterns indicate distinct features beyond the existing asthma phenotypes.

In a previous study that explored asthma phenotypes based on airway remodeling patterns on CT images, CT phenotypes showed a correlation with clinical features of severe asthma. However, its interpretation was limited due to its retrospective design.[16] This study uses QCT imaging techniques to identify asthma clusters that correlate with the clinical characteristics and varying degrees of airway remodeling observed in asthmatics. We further investigate whether each cluster shows unique responses to bronchodilator administrations in large and/or small airways.

MATERIALS AND METHODS

Study subject data

This prospective cross-sectional study included 74 patients with severe and non-severe asthma who visited allergy specialists at a tertiary referral hospital for at least 1 year from April to July 2013 (Fig. S1). The asthma diagnosis was confirmed by 2 allergy specialists based on the medical history, the presence of either bronchial reversibility (defined as an increase in forced expiratory volume in 1 s (FEV_1) of $>$12% and $>$200 mL from baseline after 400 μg of salbutamol or 4 weeks of anti-inflammatory treatment), or bronchial hyperresponsiveness (defined as a 20% drop in FEV_1 (PC_{20}) of after $<$16 mg/mL of methacholine inhalation).[16] The criteria of severe asthma were defined according to ERS/ATS guidelines.[17] Patients were excluded if they experienced an acute exacerbation event within 1 month, had active infections such as pneumonia and active tuberculosis, and had a history other chronic respiratory diseases such as interstitial lung disease or bronchiectasis. Acute asthma exacerbations were defined as an outpatient visit to the hospital and/or inpatient treatment for worsening asthma symptoms accompanied by a decrease in FEV1 $\geq$15% or required systemic steroids symptom relief.

All patients underwent spirometry with pre-bronchodilator (pre-BD) and post- bronchodilator (post-BD) tests before CT scanning. A skin prick test for 10 common inhalant allergens, induced sputum analysis, fractional exhaled nitric oxide (FeNO) test, and flexible rhinoscopy were performed. Cytokine levels (interleukin (IL)-4, IL-5, IL-8, IL10, IL-13, IL-17, basic fibroblast growth factor, interferon-γ, transforming growth factor β, periostin, and chitinase) were measured from collected serum samples (Supplemental Methods). The study protocol was approved by the institutional review

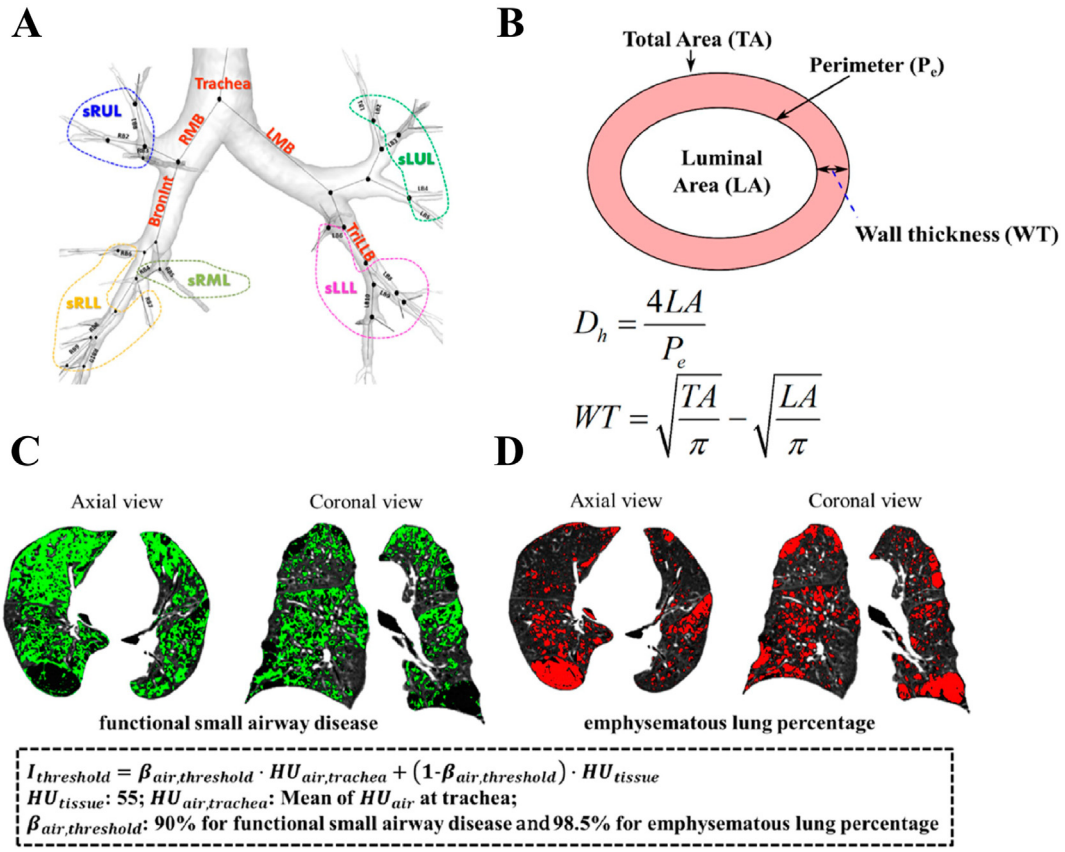

Fig. 1 Schematics of 5 large and 5 sub-grouped airways (A), hydraulic diameter and wall thickness (B), functional small airway disease (C), and emphysematous lung (D)

board of Seoul National University Hospital (IRB No. IRB No. H-0505-148-013) and informed consent was obtained from all the patients.

Computed tomography image acquisition and analysis

Chest CT imaging was performed using a 128 multi-detector CT scanner (Ingenuity, Philips Healthcare, Best, Netherlands) under full inspiration and full expiration coached by radiology technicians to obtain 2 sets of inspiratory and expiratory images for pre-BD and post-BD evaluation. CT parameters were as follows: 120 kVp tube voltage, 170 reference mAs tube current, z-dome, three-dimensional (3D) dose modulation, 1.0 mm slice thickness, 1.0 mm reconstruction increment, YC 0 reconstruction filter, 0.5 s rotation time. For quantitative analysis, all CT images were analyzed using Apollo Workstation (VIDA Diagnostics, Coralville, IA), along with a post-process algorithm that included the image registration method used to determine a spatial transformation that matches the 2 images by minimizing the sum of squared tissue volume difference Fig. 1).[18,19]

We extracted airway structural variables including the luminal wall thickness (WT) and hydraulic diameter (D_h) of 5 large airways and 5 grouped-segmental airways (Fig. 1A and B). WT and D_h were normalized by predicted values from healthy subjects[11] and were denoted as WT* and D_h*, respectively. Information regarding variables of the lung parenchyma, including functional small airway disease lung (fSAD, Fig. 1C) and emphysematous lung (Emph, Fig. 1D), were extracted. The fSAD was calculated by subtracting of the emphysema portion at inspiration from the air-trapping portion at expiration (Supplemental Methods).[20] The change rates of D_h* and fSAD% between pre- and post-BD based on post-BD values were calculated as

[D_h* (Post) − D_h* (Pre)]/D_h* (Post) and – [fSAD% (Post) − fSAD% (Pre)].

Visual analysis by radiologists

Two thoracic radiologists blinded to the patients' clinical information conducted visual analyses of the airway remodeling patterns of CT images as previously described.[16] The main level of airway remodeling was assessed according to the following criteria: "near normal type" (NN) if no remarkable abnormalities were observed, "large airway disease type" (LA) if the trachea, lobar, segmental, or subsegmental bronchi were mainly involved, and "small airway and emphysema predominant type" (SA) if air-trapping was observed distal to the subsegmental bronchi or if emphysematous changes in the lung parenchyma were observed (Fig. S2).

Clustering and statistical analyses

To obtain clustering analysis-based groups comparable to the grouping conducted by the radiologists, we included only 4 imaging-based metrics of proximal airway (WT* and D_h*) and parenchymal structures (fSAD% and Emph%) obtained post-BD. The reduced number of variables derived from principal component analysis (PCA) was used to test the *K*-means and hierarchical clustering methods. The stability of the clustering membership was evaluated by non-parametric bootstrapping analysis[21] by changing the number of clustering membership. To compare asthma clusters with healthy subjects, propensity score matching (PSM) was performed for 61 asthma and 122 healthy subjects in order to reduce the confounding effects of age, sex, body mass index, and smoking history. To validate PSM, we used standardized difference and defined balance as an absolute value less than 10.[22] Statistical analysis was performed with *R 3.6* software (Supplemental Methods).[23]

RESULTS

Characteristic lung imaging metrics of 4 QCT-based clusters

From the 74 enrolled subjects, 33 severe and 28 non-severe asthmatic patients were included in our clustering analysis and were grouped into 4 different clusters (C1 to C4). The reasons for excluding patients from the study are described in Fig. S1. Results of the principal component and clustering analyses are described in Supplemental Results.

The imaging-based clusters were primarily grouped based on proximal airway dimensions of WT* and D_h* measured at segmental levels of airways (Fig. 2A and B, and Table S2). C1 and C2 had an increase in WT* with relatively greater (C1, mean ± standard deviation: 0.329 ± 0.020) and similar (C2, 0.288 ± 0.022) D_h*, whereas C3 and C4 showed a remarkable decrease in D_h* (C3: 0.233 ± 0.025; C4: 0.247 ± 0.018, respectively) without airway wall thickening when compared to healthy subjects (Table S2). Although fSAD% was noticeably increased in both C1 and C4, prominent Emph% was detected only in C4 (12.2 ± 5.8%, $P < 0.005$) (Fig. 2C and D, and Table S2). C2 and C3 showed no noticeable increases in fSAD% and Emph%. Fig. 2E and F highlight the CT-based characteristics between clearly separated clusters through visualizing the 2D distribution for D_h* and fSAD% as well as the 3D distribution for D_h*, fSAD %, and Emph%.

To measure the dynamic change of D_h* and fSAD % between pre- and post-BD, we compared the ΔD_h*/D_h* and ΔfSAD% values (Fig. 3A and B, and Table S3). Distal airways of C1 were least responsive as represented by the small ΔfSAD% when compared to that of C3 (median [interquartile ranges]: 8.4 [2.2–15.1] *vs.* −2.0 [−4.8-(-1.0)], $P = 0.007$). While C1 showed a relatively conserved bronchodilator response in terms of the D_h* of proximal segmental airways, C2 demonstrated a relatively greater improvement in D_h* at post-BD compared to C3 (0.118 [0.065–0.160] *vs.* 0.040 [−0.023-0.073], $P = 0.005$). The dynamic change of D_h* and fSAD% indicate that good bronchodilator responses were observed in the proximal airways of C2 and in distal small airways of C3 (Fig. 3C and D). In contrast, subjects in C4 were unresponsive to bronchodilator administration at both proximal and distal airway levels.

Clinical characteristics of 4 QCT-based clusters

A greater number of severe asthmatic subjects were included in C3 and C4 (81.3% and 100%) compared to C1 and C2 (14.2% and 42.4%)

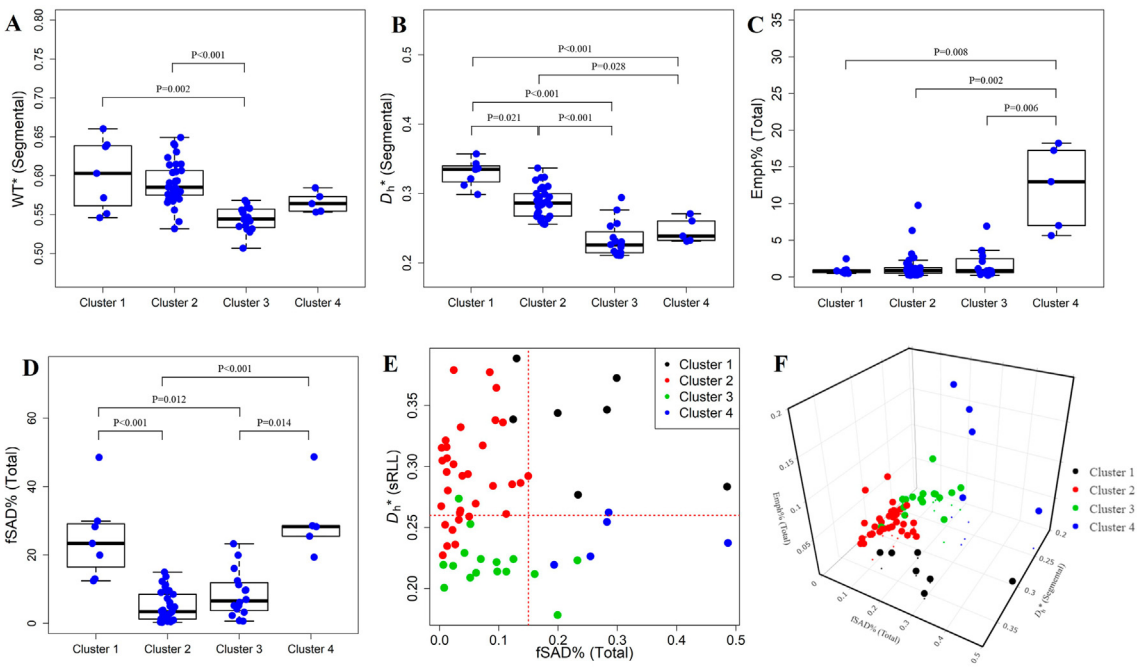

Fig. 2 Comparison of CT-based quantitative metrics between clusters at post-bronchodilator for (A) normalized wall thickness (WT*); (B) normalized hydraulic diameter (D_h*); (C) functional small airway disease percentage (fSAD%); (D) emphysematous lung percentage (Emph %); (E) 2D distribution of clusters according to D_h* and fSAD%; (F) 3D distribution of clusters according to D_h*, fSAD%, and Emph%

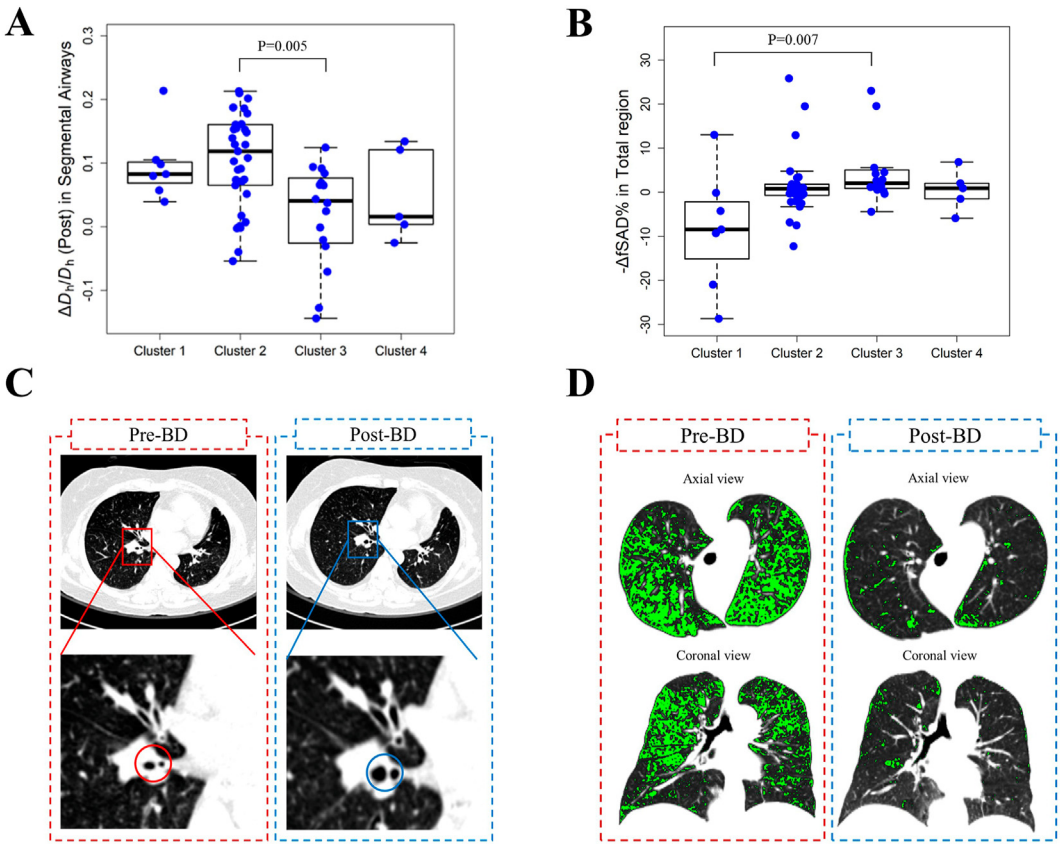

Fig. 3 The rate of change between pre- and post- bronchodilators was computed as (A) [D_h* (Post) – D_h* (Pre)] / D_h* (Post); (B) – [fSAD% (Post) - fSAD% (Pre)]. The representative images of the change of D_h* in cluster 2 (C) and fSAD% in cluster 3 (D) between pre- and post-bronchodilators

($P < 0.005$), and accordingly, patients in C3 and C4 used a higher number of controller medications and oral corticosteroids (OCS) (Table 1). Subjects in C1 included older females with late-onset asthma and no previous smoking history. The lung functions of C1 subjects were within the normal range irrespective of bronchodilator treatment, and the total serum IgE level was the lowest among the 4 clusters. C2 included relatively younger females with early asthma onset and 27.3% were receiving OCS treatment. Subjects in C3 were characterized by high total IgE levels with a slight reduction of FEV_1/FVC and FEV_1 in both pre- and post-BD. C4 included males with severe asthma and a previous smoking history with the highest pack-years compared to other clusters. These patients were highly sensitive to the methacholine challenge test with lowest PC_{20} value at diagnosis and had the most severely reduced post-BD FEV_1/FVC (55.2 ± 4.3%) and FEV_1 (57.4 ± 11.8%).

The distinct clinical features for each cluster are summarized in Fig. 4. The average annual number of exacerbations per subject over a follow-up period of up to 5 years increased from C1 (0.2 [0.1–0.4] per year) and C2 (0 [0–0.5] per year) to C3 (0.4 [0.2–0.8] per year) and C4 (1.0 [0.3–1.5] per year) ($P < 0.05$). The rate of fixed obstruction was similar to the pattern of acute exacerbations, increasing from C1 to C4. The degree of airway hyper-responsiveness showed a similar worsening as post-BD FEV_1/FVC did from C1 to C4.

However, the percentage of sputum eosinophils and neutrophils, FeNO, and various serum cytokine levels did not show any significant difference among the 4 QCT-based clusters (Table 1 and Table S4).

Comparison of grouping by clustering-based groups vs. radiologists

Based on CT-based airway remodeling patterns visually inspected by experienced radiologists, the study subjects were classified into 3 different groups: NN type, LA type, and SA type. Details of the quantitative assessment and clinical features are reported in the Supplemental Results. Although the 3 groups demonstrated similar WT* values, the D_h* values measured at the segmental bronchi level were significantly decreased in LA and SA types compared to that of the NN type (NN: 0.288 ± 0.033; LA: 0.252 ± 0.032; and SA: 0.256 ± 0.048, $P < 0.005$). Emph% was noticeably greater in the SA type than in the NN and LA types, and the LA type demonstrated a moderately increased Emph% compared to the NN type (NN: 1.1 ± 1.2%; LA: 1.9 ± 1.9%; and SA: 13 ± 4.8%, $P < 0.001$). The SA type had an increased fSAD% compared to NN and LA types (NN: 8.7 ± 10.5%; LA: 11.1 ± 11.8%; and SA: 18.2 ± 9%, $P = 0.064$) (Table 2). All subjects in the SA group were male and had a history of smoking, while those in the other groups were predominantly non-smoking females. No significant differences were observed among the 3 groups in terms of age, disease onset, duration, body mass index, and presence of sinusitis or nasal polyps (Table 3). The proportion of patients with severe asthma in the NN, LA, and SA types were 36.8%, 77.8%, and 100%, respectively ($P < 0.005$). Reductions in FEV_1/FVC and FEV_1 were more prominent in the LA and SA types than in NN type ($P < 0.001$). While fixed airflow obstruction (defined as $FEV_1 < 70\%$ and FEV_1/FVC <70% despite bronchodilator inhalation) was not observed in the NN type, it was relatively common in the LA and SA types (NN: 0%; LA: 33.3%; and SA: 60%, $P < 0.001$).

A significant association was found between the grouping done by radiologists and that done by the clustering analysis ($R = 0.533$, $P < 0.001$) (Fig. 5). However, the clustering analysis approach provided more detailed data. For example, the clustering analysis-based grouping further divided the NN subjects into the 3 different clusters (C1, C2, and C3). The LA dominant subjects were mostly included in C2 and C3. Although the SA dominant subjects were also divided into the 3 clusters, 60% converged to C4. In the aspect of clusters, C1 was entirely comprised of the NN type. The NN and LA type proportions of C2 were 69.7% and 27.3%, and 50% and 43.8% for C3, respectively. Among the 4 clusters, C4 had the highest proportion of the SA type at 60%, and the LA type comprised the remaining 40%. No subjects belonging to the NN type were included in C4.

Clinical characteristics	Cluster 1 (N = 7)	Cluster 2 (N = 33)	Cluster 3 (N = 16)	Cluster 4 (N = 5)	*P* value
Asthma severity (Severe)	1 (14.2%)	14 (42.4%)	13 (81.3%)	5 (100%)	<0.005
Age (y)	74.0 [64.5; 77.0]	62.0 [53.0; 68.0]	69.0 [62.5; 74.5]	67.0 [63.0; 68.0]	<0.05
Onset age of asthma (y)	59.0 [54.0; 65.0]	46.0 [36.0; 55.0]	54.0 [44.3; 62.0]	54.0 [40.0; 59.0]	<0.05
Disease duration (y)	11.0 [09.0; 12.5]	12.0 [09.0; 19.0]	14.0 [09.8; 17.0]	17.0 [14.0; 23.0]	0.463
Sex (female)	7 (100%)	26 (78.8%)	7 (43.8%)	0 (0%)	<0.001‡,‖
Smoking status (Never/Former/Current)	7/0/0 (100/0/0%)	26/5/2 (79/15/6%)	11/4/1 (69/25/6%)	0/5/0 (0/100/0%)	<0.005‖
Smoking history (pack-years)	0	4.9 ± 15.0	7.5 ± 11.7	35 ± 23.0	<0.001§,‖,¶
BMI (kg/m^2)	23.7 ± 2.5	25.0 ± 3.2	24.0 ± 1.7	23.0 ± 1.4	0.3
Sinusitis	4 (56.8%)	19 (57.6%)	12 (75%)	3 (60%)	0.682
Nasal polyp	0 (0%)	4 (12.1%)	4 (25%)	0 (0%)	0.281
Atopy	1 (14.2%)	10 (30.3%)	6 (37.5%)	1 (20%)	0.683
Total IgE (IU/ml)	30.0 [4.0; 45.0]	88.0 [37.0; 192.0]	441.0 [69.5; 1099.5]	31.0 [30.0; 40.0]	<0.05
Sputum eosinophil (%)	4.0 [3.7; 4.3]	4.1 [3.0; 8.4]	6.3 [3.0; 14.7]	10.0 [9.2; 11.5]	0.607
Sputum neutrophil (%)	11.0 [5.8; 17.3]	1.3 [0.8; 2.8]	1.0 [0.4; 3.0]	1.0 [0.7; 1.3]	0.858
FeNO (ppb)	9.5 (7.8)	27.8 (16.0)	24.5 (14.0)	20.3 (15.0)	0.353
PC_{20} (mg/ml, at diagnosis)	21.0 [7.4; 22.0]	6.7 [3.5; 15.2]	3.4 [2.0; 7.6]	0.6 [0.3; 1.1]	<0.01§,‖
Pre-BD FVC (%pred)	93.0 ± 22.5	78.2 ± 16.0	67.9 ± 22.6	75.4 ± 15.3	0.152
Pre-BD FEV_1 (%pred)	105 ± 24.8	80.5 ± 17.3	67.3 ± 20.8	52.6 ± 12.5	<0.001†,§,‖
Pre-BD FEV_1/FVC (%)	91.0 ± 3.7	84.7 ± 7.6	74.1 ± 11.8	57.2 ± 5.8	<0.001†,‡,§,‖
Post-BD FVC (%pred)	94.3 ± 23.7	82.2 ± 14.5	71.8 ± 15.2	85.6 ± 18.7	0.072
Post-BD FEV_1 (%pred)	109 ± 25.6	86.1 ± 17.6	71.4 ± 19.9	57.4 ± 11.8	<0.001†,‡,§,‖
Post-BD FEV_1/FVC (%)	93.6 ± 4.7	85.3 ± 6.8	75.6 ± 12.6	55.2 ± 4.3	<0.001*,†,‡,§,‖
Fixed obstruction**	0 (0%)	1 (3%)	4 (25%)	4 (80%)	<0.001§
No. of controller medications	1.3 ± 0.8	1.4 ± 0.9	2.3 ± 1.2	2.6 ± 1.5	<0.05
Maintenance of OCS (%)	2 (28.6%)	9 (27.3%)	10 (62.5%)	4 (80%)	<0.05
No. of acute exacerbations (per year, 2012–2017)	0.2 [0.1; 0.4]	0.0 [0.0; 0.5]	0.4 [0.2; 0.8]	1.0 [0.3; 1.5]	<0.05

Table 1. Clinical characteristics of the 4 CT imaging-based clusters derived by the clustering analysis. *Abbreviations: BMI, body mass index; FeNO, fractional exhaled nitric oxide; Pre-BD, pre-bronchodilator; Post-BD, post-bronchodilator; BDR, bronchodilator response; OCS, oral corticosteroids. Values are presented as mean ± standard deviation, or median [25% quartile; 75% quartile], or number (%). Kruskal–Wallis and χ^2 tests with Dunn's and Bonferroni post hoc tests for continuous and categorical variables were performed for "populations: Cluster 1 vs. Cluster 2 vs. Cluster 3 vs. Cluster 4". *P < 0.05 for Cluster 1 vs. Cluster 2. †P < 0.05 for Cluster 1 vs. Cluster 3. ‡P < 0.05 for Cluster 2 vs. Cluster 3. §P < 0.05 for Cluster 1 vs. Cluster 4. ‖P < 0.05 for Cluster 2 vs. Cluster 4. ¶P < 0.05 for Cluster 3 vs. Cluster 4. **Fixed obstruction: FEV_1 <70% and FEV_1/FVC <70% despite bronchodilator application*

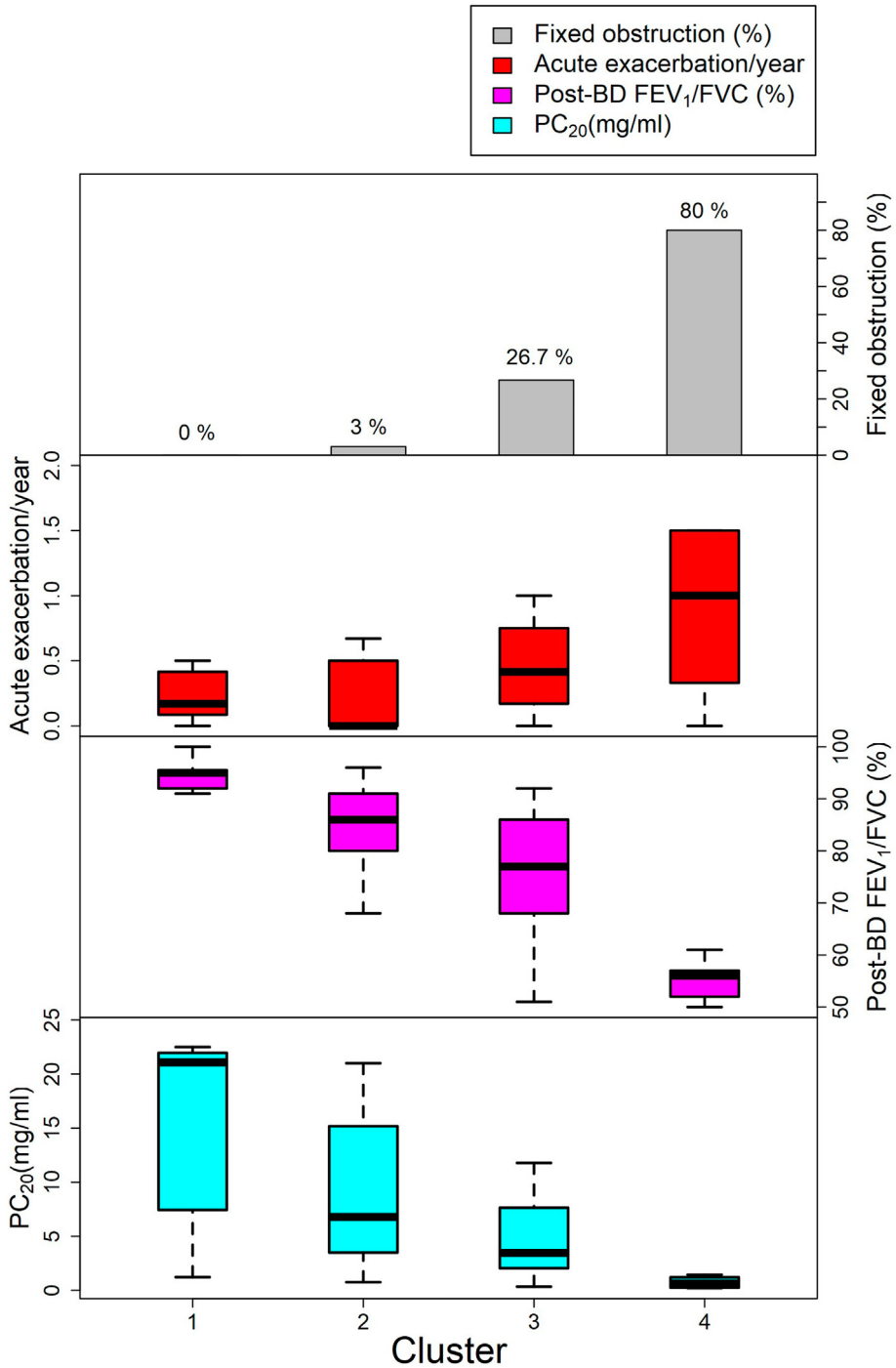

Fig. 4 Representative clinical characteristics of the 4 QCT imaging-based clusters

DISCUSSION

This study was conducted to determine whether QCT metrics of airway and parenchymal structure can be used to group asthmatic patients into clinically and physiologically distinct phenotypes. As this was a prospectively designed study, a collaborative effort was made among clinicians, radiologists, and engineers to maintain consistent imaging protocols. This study is novel in that CT images taken consistently within a short period of time were independently evaluated by radiologists and computer scientists, and data collected from

CT-based metrics		NN type (N = 38)	LA type (N = 18)	SA type (N = 5)	*P* value	Healthy subjects
WT*	Trachea	1.014 ± 0.082	1.010 ± 0.077	1.040 ± 0.043	0.685	0.970 ± 0.093
	RMB	0.936 ± 0.150	0.919 ± 0.156	1.013 ± 0.039	0.662	0.857 ± 0.143
	Bronint	0.688 ± 0.062	0.683 ± 0.045	0.677 ± 0.039	0.966	0.671 ± 0.061
	LMB	0.719 ± 0.099	0.730 ± 0.109	0.822 ± 0.164	0.304	0.724 ± 0.105
	TriLLB	0.667 ± 0.052	0.681 ± 0.082	0.640 ± 0.036	0.338	0.632 ± 0.041
	sRUL	0.601 ± 0.044	0.590 ± 0.039	0.601 ± 0.019	0.755	0.573 ± 0.037
	sRML	0.575 ± 0.051	0.569 ± 0.045	0.550 ± 0.052	0.763*	0.551 ± 0.038
	sRLL	0.583 ± 0.045	0.559 ± 0.032	0.578 ± 0.031	0.152	0.552 ± 0.041
	sLUL	0.558 ± 0.029	0.537 ± 0.032	0.540 ± 0.021	<0.05	0.526 ± 0.039
	sLLL	0.602 ± 0.042	0.584 ± 0.040	0.573 ± 0.018	0.175	0.572 ± 0.039
	Total§	0.584 ± 0.037	0.568 ± 0.030	0.569 ± 0.016	0.295	0.555 ± 0.032
D_h*	Trachea	0.987 ± 0.100	1.021 ± 0.068	0.944 ± 0.061	0.092	0.916 ± 0.089
	RMB	0.825 ± 0.079	0.795 ± 0.050	0.752 ± 0.055	0.055	0.766 ± 0.087
	Bronint	0.607 ± 0.052	0.618 ± 0.053	0.613 ± 0.056	0.885	0.579 ± 0.056
	LMB	0.668 ± 0.073	0.653 ± 0.052	0.655 ± 0.032	0.834	0.615 ± 0.065
	TriLLB	0.486 ± 0.059	0.447 ± 0.076	0.411 ± 0.062	<0.05	0.441 ± 0.058
	sRUL	0.313 ± 0.043	0.278 ± 0.044	0.302 ± 0.062	<0.05*	0.282 ± 0.038
	sRML	0.273 ± 0.041	0.248 ± 0.042	0.233 ± 0.052	0.127	0.257 ± 0.039
	sRLL	0.288 ± 0.047	0.249 ± 0.047	0.260 ± 0.067	<0.01*	0.267 ± 0.044
	sLUL	0.242 ± 0.029	0.216 ± 0.032	0.224 ± 0.038	<0.05*	0.232 ± 0.030
	sLLL	0.325 ± 0.045	0.268 ± 0.041	0.259 ± 0.038	<0.001	0.290 ± 0.040
	Total§	0.288 ± 0.033	0.252 ± 0.032	0.256 ± 0.048	<0.005*	0.266 ± 0.031
Emph%	RUL	1.0 ± 1.0	1.4 ± 1.9	17.1 ± 10.3	<0.001†,‡	0.7 ± 1.4
	RML	1.8 ± 1.9	2.6 ± 2.1	5.8 ± 1.4	<0.001†,‡	1.9 ± 3.0
	RLL	0.8 ± 1.3	1.2 ± 1.0	11.0 ± 7.3	<0.001*,†,‡	0.8 ± 1.3
	LUL	1.2 ± 1.4	2.4 ± 2.7	17.0 ± 5.5	<0.001*,†,‡	1.1 ± 2.0
	LLL	1.0 ± 1.2	2.3 ± 2.6	11.6 ± 4.4	<0.001†,‡	1.0 ± 1.4
	Total	1.1 ± 1.2	1.9 ± 1.9	13.0 ± 4.8	<0.001†,‡	1.0 ± 1.6
fSAD%	RUL	9.9 ± 12.1	10.6 ± 15.1	25.4 ± 10.6	<0.05†,‡	10.9 ± 13.9
	RML	20.1 ± 16.5	25.6 ± 15.3	32.1 ± 19.1	0.187	19.9 ± 17.7
	RLL	3.8 ± 8.6	6.9 ± 8.9	11.1 ± 10.0	<0.01*,†	3.9 ± 7.2
	LUL	11.9 ± 14.3	12.6 ± 12.6	23.0 ± 9.2	0.086	12.1 ± 14.9
	LLL	4.6 ± 9.6	8.6 ± 11.2	9.6 ± 6.6	<0.05†	3.3 ± 6.2
	Total	8.7 ± 10.5	11.1 ± 11.8	18.2 ± 9.0	0.064	8.7 ± 10.5

Table 2. CT-based quantitative metrics in 3 visually assessed asthma phenotypes (near normal [NN], large airway disease [LA], and small airway disease [SA]). *Abbreviations: WT*, normalized luminal wall thickness; D_h*, normalized hydraulic diameter; Emph, emphysema; fSAD, functional small airway disease; RMB, right main bronchus; Bronint, intermediate bronchus; LMB, left main bronchus; TriLLB, trifurcation of left lower bronchus; sRUL, averaged in segmental airways of right upper lobe; sRML, averaged in segmental airways of right middle lobe; sRLL, averaged in segmental airways of right lower lobe; sLUL, averaged in segmental airways of left upper lobe; sLLL, averaged in segmental airways of left lower lobe. Values are presented as mean ± standard deviation. Kruskal–Wallis tests with Dunn's post hoc tests were performed for "populations: NN type vs. LA type vs. SA type." *P < 0.05 for NN type vs. LA type. †P < 0.05 for NN type vs. SA type. ‡P < 0.05 for LA type vs. SA type. §Total indicates the average of segmental airways. Reference values of healthy subjects were balanced for age, sex, body mass index, history of smoking, and pack-years with asthma cohort using propensity score matching methods*

Machine learning-based grouping	Grouping by radiologists			All
	NN	LA	SA	
Cluster 1	7	0	0	7
Cluster 2	23	9	1	33
Cluster 3	8	7	1	16
Cluster 4	0	2	3	5
All	38	18	5	61

Fig. 5 Association between clustering-based grouping and grouping by radiologists. *Size of each dot plot indicates the average percentage of each type classified by radiologists in that cluster

these images were assessed in collaboration across various disciplines.

Several previous studies defined clinical clusters of asthma based on demographic features, pulmonary function test (PFT) results and laboratory data in order to understand the pathophysiology behind heterogeneous asthma.[24–27] In addition, the assessment of airway structural and functional remodeling using QCT in asthmatic patients has provided a new means for asthma phenotyping.[28,29] While the QCT clustering method used in this study shares similarities with the approach previously proposed by the study based on the severe asthma research program (SARP),[28] our study has a unique prospective design where radiologists made diagnoses and 2 sets of inspiratory and expiratory CT images for pre-bronchodilator (BD) vs post-BD were obtained. In addition, the current study used only 4 parameters including WT*, D_h*, fSAD%, and Emph % to make associations between the radiologists' visual analysis and BD responses. These metrics indicate the degree of wall thickening of large airways, narrowing of large airways, narrowing of small airways, and parenchymal tissue destruction, respectively.

The 2 clusters identified in this study were similar to the clusters identified in SARP. For example, subjects in cluster 2 based on SARP and cluster 3 of the current study predominantly showed airway narrowing without airway wall thickening and both clusters demonstrated persistent alteration of lung function. Subjects in cluster 4 of SARP and cluster 4 of the current study showed airway narrowing and air-trapping features, and these clusters mostly included severe asthmatic males with symptoms of asthma and chronic obstructive pulmonary disease (COPD) overlap (ACO). Meanwhile, our study could not identify the obese, female-dominant severe asthma group previously classified by SARP. Such similarities and differences between the results of our study and SARP show that direct comparisons among clusters may be limited as the clinical setting, genetic backgrounds, and socio-environmental effects of the 2 studies are different. Thus, a prospective study that includes a multi-ethnic asthma population is needed to gain a better understanding of the imaging phenotypes.

In our study, we followed the normalization scheme of a previous study[11] to eliminate inter-subject variability caused by sex, age, height, and confirmed increases in WT* or decreases in D_h* commonly found among Korean asthmatics. The decrease D_h* was the most representative structural change that was correlated with alterations of clinical and PFT-based functional variables.[11,28] These findings are buttressed by the results of previous studies which showed that luminal narrowing is a prominent feature of proximal airway remodeling in asthmatic patients.[29,30] Meanwhile, mild bronchial dilatation is observed 15–77% of patients with uncomplicated asthma,[31] and similar results were observed in our study: relatively larger D_h* values were observed in patients belonging to C1 in comparison to other clusters. Although mild bronchial dilatation may be a relatively common finding reported in 15–77% of patients with uncomplicated asthma,[31] it can be disguised by numerous variables including mucus impaction, reduction in pulmonary artery diameter and air-trapping.[32]

During inspiration, the fSAD% increases due to air trapping. Interestingly, the results of our study show that C1 and C4 persistently had increased fSAD% despite bronchodilator administration. C1 represents the clinical phenotype of mild asthma, and is characterized by air-trapping without emphysema or detectable narrowing of the airways. As C4 included patients with a history of heavy smoking, the presence of emphysema distinguished it from C1. Unlike previous studies that excluded smokers, our study provides a more comprehensive clustering analysis and may better

Clinical characteristics	NN type (N = 38)	LA type (N = 18)	SA type (N = 5)	*P* value
Asthma severity (Severe)	14 (36.8%)	14 (77.8%)	5 (100%)	<0.005*
Age (y)	66.5 [57.0; 74.0]	63.0 [56.0; 67.0]	68.0 [53.0; 76.0]	0.574
Onset age of asthma (y)	53.0 [42.0; 62.0]	46.5 [40.0; 56.0]	54.0 [44.0; 59.0]	0.548
Disease duration (y)	11.0 [9.0; 17.0]	15.0 [13.0; 23.0]	14.0 [14.0; 17.0]	0.324
Sex (female)	29 (76.3%)	11 (61.1%)	0 (0%)	<0.005†
Smoking status (Never/Former/Current)	32/6/0 (84.2/15.8/0%)	12/5/1 (66.7/27.8/5.6%)	0/3/2 (0/60/40%)	<0.001†
BMI (kg/m^2)	24.6 ± 3.1	24.4 ± 1.9	23.3 ± 2.4	0.794
Sinusitis	22 (57.9%)	12 (66.7%)	4 (80%)	0.656
Nasal polyp	4 (10.5%)	4 (22.2%)	0 (0%)	0.323
Atopy	12 (31.6%)	5 (27.8%)	1 (20%)	1.000
Total IgE (IU/ml)	62.0 [27.0; 145.0]	94.0 [40.0; 469.0]	42.0 [30.5; 886.5]	0.491
Sputum eosinophil (%)	3.3 [3.0; 5.0]	9.3 [4.8; 17.7]	7.7 [5.0; 10.2]	<0.05*
Sputum neutrophil (%)	1.0 [0.7; 3.7]	1.2 [0.5; 2.5]	3.0 [2.3; 5.7]	0.263
FeNO (ppb)	23.7 ± 14.2	28.9 ± 17.8	22.2 ± 13.9	0.372
PC_{20} (mg/ml, at diagnosis)	9.3 [3.6; 16.8]	5.3 [2.0; 13.3]	1.4 [1.0; 1.4]	<0.05†
Pre-BD FVC (%pred)	81.3 ± 22.1	69.1 ± 10.5	72.8 ± 16.2	<0.05*
Pre-BD FEV_1 (%pred)	87.6 ± 21.0	62.7 ± 14.8	54.8 ± 10.3	<0.001*,†
Pre-BD FEV_1/FVC (%)	85.3 ± 7.8	74.9 ± 14.3	62.4 ± 3.9	<0.001*,†
Post-BD FVC (%pred)	84.6 ± 17.9	75.0 ± 12.2	78.2 ± 21.4	0.15
Post-BD FEV_1 (%pred)	91.9 ± 21.2	69.1 ± 15.4	57.8 ± 10.9	<0.001*,†
Post-BD FEV_1/FVC (%)	87.0 ± 7.1	74.6 ± 14.5	61.8 ± 8.2	<0.001*,†
Fixed obstruction§	0 (0%)	6 (33.3%)	3 (60%)	<0.001*,†
No. of controller medications	1.5 ± 1.0	2.1 ± 1.1	2.2 ± 1.3	<0.05
Maintenance of OCS (%)	11 (28.9%)	11 (61.1%)	3 (60%)	<0.05
No. of acute exacerbations (per year, 2012–2017)	0.1 [0.0; 0.3]	0.4 [0.0; 0.7]	0.7 [0.5; 1.0]	<0.05

Table 3. Clinical characteristics between visually assessed asthma phenotypes (near normal [NN], large airway disease [LA], and small airway disease [SA]). *Abbreviations: BMI, body mass index; FeNO, fractional exhaled nitric oxide; Pre-BD, pre-bronchodilator; Post-BD, post-bronchodilator; BDR, bronchodilator response; OCS, oral corticosteroids. Values are presented as mean ± standard deviation, or median [25% quartile; 75% quartile] or number (%). Kruskal–Wallis and χ^2 tests with Dunn's and Bonferroni post hoc tests for continuous and categorical variables were performed for populations: NN type vs. LA type vs. SA type". *P < 0.05 for NN type vs. LA type. †P < 0.05 for NN type vs. SA type. §Fixed obstruction: FEV_1 <70% and FEV_1/FVC <70% despite bronchodilator application*

reflect real-world practices. ACO is now widely accepted as a distinct clinical entity on the basis that asthma and COPD are heterogeneous diseases.[33-35] ACO is associated with noxious exposure such as smoking and is characterized by persistent airflow limitation and frequent exacerbations.[36-38] These features are consistent with the clinical characteristics observed in C4.

We identified distinct dynamic changes of 4 imaging-derived phenotypes that had different effects of bronchodilator on the D_h* of segmental airways and non-emphysematous air-trapping component (fSAD%) of small airways.[39,40] While the bronchodilator response was limited in C3 and C4, patients in C2 typically showed good bronchodilator responses in both large and small airways. The D_h* of proximal airways showed diminished bronchodilator responsiveness in C3 and C4, and these clusters also exhibited a higher degree of fixed airflow obstruction and had more frequent asthma exacerbations. These findings show that QCT-based clusters may serve as a complementary tool for assessing clinical outcomes.

Clustering using CT metrics not only showed a significant association with the grouping done by radiologists, but also provided information beyond what was obtained through visual inspection. For example, QCT-based clustering allowed for more sensitive detection of airway remodeling in patients who showed no abnormal findings on visual inspection of CT images. These clusters identified with the QCT method were closely related to clinical outcomes such as reduced lung function and acute exacerbations. As such, imaging analysis allows for the understanding of structural pathologies complementary to the clinical data and pulmonary function of the existing asthma phenotypes.

A recent study of severe asthma patients from the U-BIOPRED cohort showed that subjects with persistent airflow limitation had distinct gene expression profiles associated with treatment, inflammatory pathways, and airway remodeling that distinguished them from the control group.[41] To our knowledge, there has been no study that analyzed tissue transcriptomes among CT-derived clusters of asthma. In this study, each QCT-based cluster showed differences in clinical features such as age, sex, asthma onset, smoking history, serum total IgE, and PC_{20}, and this suggests that these clusters represent distinct asthma phenotypes. To investigate whether airway remodeling patterns were affected by differential cytokine expression, we measured various serum cytokines in all subjects. However, no significant differences were found among clusters (Table S4). Future studies using tissue samples may help us to gain a better understanding of the underlying mechanism of CT-based phenotypes.

This study has several limitations. First, the sample size was relatively small to draw a conclusion, especially in the cluster 4 and SA type. However, the SA type was not commonly encountered among severe asthma. In the previous retrospective study, only 6.6% of 91 patients with severe asthma exhibited SA type, which was the least common among 4 severe asthma phenotypes.[16] A replication study based on the multicenter study with a larger number of asthmatics is needed to validate the findings of this study. Second, the use of asthma medications was not restricted. As all patients enrolled in the study continued to receive ongoing treatment that included inhaled corticosteroids, OCS, and antihistamines, the use of these medications may have impacted the sputum eosinophil count, atopic status, FeNO, and serum cytokine levels. While the confounding effects of asthma treatment may have affected measured variables, these effects make the results of our study more applicable for clinical use where patients receive unrestricted treatment.

We identified 4 distinct clusters based on QCT imaging in adult Korean patients with asthma. We found that the unique structural and functional changes observed in each cluster were associated with distinct clinical characteristics and outcomes. QCT-based clustering is a sensitive method for the detection of airway remodeling and can provide useful prognostic data for asthma phenotypes.

Abbreviations

ACO: asthma-chronic obstructive pulmonary disease overlap; BMI: body mass index; COPD: chronic obstructive pulmonary disease; CT: computed tomography; D_h: hydraulic diameter; FeNO: fractional exhaled nitric oxide; FEV_1: forced expiratory volume in 1 second; fSAD: functional small airway disease; FVC: forced vital capacity; OCS: oral corticosteroid; PCA: principal component analysis; PFT: pulmonary function test; QCT: quantitative computed tomography; SARP: severe Asthma Research

Program; sRUL: averaged in segmental airways of right upper lobe; sRML: averaged in segmental airways of right middle lobe; sRLL: averaged in segmental airways of right lower lobe; sLUL: averaged in segmental airways of left upper lobe; sLLL: averaged in segmental airways of left lower lobe; WT: airway wall thickness.

Financial support
This work was supported in part by National Research Foundation of Korea (NRF) grant funded by Korea government [grant numbers 2016R1D1A1B03936078 and 2017R1D1A1A09082160] and Korea Environment Industry & Technology Institute (KEITI) through an Environmental Health Action Program funded by Korea Ministry of Environment (MOE) [grant number 2018001360001].

Authors' contributions
Conceived and designed the study: C-H Lee and H-R Kang, Data analysis and manuscript writing: S Kim and S Choi, Subject recruitment: H-R Kang and S-H Cho, Radiological phenotyping: K-N Jin and C-H Lee, Statistical analysis: T Kim.

Consent for publication
All the authors agree on publishing the submitted document.

Availability of data and materials
All data generated or analyzed during this study are available within this published article and its supporting information files.

Ethics approval
The study protocol was approved by the institutional review board of Seoul National University Hospital (IRB No. H-0505-148-013) and informed consent was obtained from all the patients.

Declaration of competing interest
The authors declare no conflict of interest.

Acknowledgments
We would like to express our sincere gratitude to Sojung Park RN for her devotion to this clinical investigation and to Yoon Hae Ahn for helping us develop the main findings of this study more clearly.

Appendix A. Supplementary data
Supplementary data to this article can be found online at https://doi.org/10.1016/j.waojou.2022.100628.

Author details
[a]Division of Allergy and Clinical Immunology, Department of Internal Medicine, School of Medicine, Kyungpook National University, Daegu, South Korea. [b]School of Mechanical Engineering, Kyungpook National University, Daegu, South Korea. [c]Department of Radiology, SMG-SNU Boramae Medical Center, Seoul, South Korea. [d]Institute of Allergy and Clinical Immunology, Seoul National University Medical Research Center, Seoul, South Korea. [e]Department of Internal Medicine, Seoul National University College of Medicine, Seoul National University Hospital, Seoul, South Korea. [f]Department of Radiology, Seoul National University College of Medicine, Seoul National University Hospital, Seoul, South Korea. [g]Institute of Radiation Medicine, Seoul National University Medical Research Center, Seoul, South Korea.

REFERENCES

1. Bai TR, Knight DA. Structural changes in the airways in asthma: observations and consequences. *Clin Sci (Lond)*. 2005;108(6):463–477.
2. Black JL, Roth M, Lee J, et al. Mechanisms of airway remodeling. Airway smooth muscle. *Am J Respir Crit Care Med*. 2001;164(10 Pt 2):S63–S66.
3. Hirota N, Martin JG. Mechanisms of airway remodeling. *Chest*. 2013;144(3):1026–1032.
4. Busse WW, Lemanske Jr RF. *Asthma. N Engl J Med*. 2001;344(5):350–362.
5. Prakash YS, Halayko AJ, Gosens R, et al. An official American thoracic society research statement: current challenges facing research and therapeutic advances in airway remodeling. *Am J Respir Crit Care Med*. 2017;195(2):e4–e19.
6. Fixman ED, Stewart A, Martin JG. Basic mechanisms of development of airway structural changes in asthma. *Eur Respir J*. 2007;29(2):379–389.
7. Busacker A, Newell Jr JD, Keefe T, et al. A multivariate analysis of risk factors for the air-trapping asthmatic phenotype as measured by quantitative CT analysis. *Chest*. 2009;135(1):48–56.
8. Choi S, Hoffman EA, Wenzel SE, et al. Improved CT-based estimate of pulmonary gas trapping accounting for scanner and lung volume variations in a multi-center study. *J Appl Physiol*. 2014;117(6):593–603, 1985.
9. Zhang XX, Xia TT, Lai ZD, et al. Uncontrolled asthma phenotypes defined from parameters using quantitative CT analysis. *Eur Radiol*. 2019;29(6):2848–2858.
10. Aysola RS, Hoffman EA, Gierada D, et al. Airway remodeling measured by multidetector CT is increased in severe asthma and correlates with pathology. *Chest*. 2008;134(6):1183–1191.
11. Choi S, Hoffman EA, Wenzel SE, et al. Quantitative assessment of multiscale structural and functional alterations in asthmatic populations. *J Appl Physiol*. 2015;118(10):1286–1298, 1985.
12. Hartley RA, Barker BL, Newby C, et al. Relationship between lung function and quantitative computed tomographic parameters of airway remodeling, air trapping, and emphysema in patients with asthma and chronic obstructive pulmonary disease: a single-center study. *J Allergy Clin Immunol*. 2016;137(5):1413–+.
13. Berair R, Hartley R, Mistry V, et al. Associations in asthma between quantitative computed tomography and bronchial biopsy-derived airway remodelling. *Eur Respir J*. 2017;49(5).
14. Walker C, Gupta S, Hartley R, et al. Computed tomography scans in severe asthma: utility and clinical implications. *Curr Opin Pulm Med*. 2012;18(1):42–47.

15. Gupta S, Hartley R, Singapuri A, et al. Temporal assessment of airway remodeling in severe asthma using quantitative computed tomography. *Am J Resp Crit Care*. 2015;191(1):107–110.
16. Kim S, Lee CH, Jin KN, et al. Severe asthma phenotypes classified by site of airway involvement and remodeling via chest CT scan. *J Investigat Allergol Clin Immunol*. 2018;28(5):312–320.
17. Chung KF, Wenzel SE, Brozek JL, et al. International ERS/ATS guidelines on definition, evaluation and treatment of severe asthma. *Eur Respir J*. 2014;43(2):343–373.
18. Yin YB, Hoffman EA, Lin CL. Mass preserving nonrigid registration of CT lung images using cubic B-spline. *Med Phys*. 2009;36(9):4213–4222.
19. Choi S, Hoffman EA, Wenzel SE, et al. Registration-based assessment of regional lung function via volumetric CT images of normal subjects vs. severe asthmatics. *J Appl Physiol*. 2013;115(5):730–742, 1985.
20. Galban CJ, Han MK, Boes JL, et al. Computed tomography-based biomarker provides unique signature for diagnosis of COPD phenotypes and disease progression. *Nat Med*. 2012;18(11):1711–1715.
21. Hennig C. *fpc: Flexible Procedures for Clustering*. 2014. R package version 2.1-9 ed.
22. Zhang Z, Kim HJ, Lonjon G, et al. Balance diagnostics after propensity score matching. *Ann Transl Med*. 2019;7(1):16.
23. Team RCR. *A Language and Environment for Statistical Computing*. R Foundation for Statistical Computing; 2013.
24. Moore WC, Meyers DA, Wenzel SE, et al. Identification of asthma phenotypes using cluster analysis in the Severe Asthma Research Program. *Am J Respir Crit Care Med*. 2010;181(4):315–323.
25. Moore WC, Hastie AT, Li X, et al. Sputum neutrophil counts are associated with more severe asthma phenotypes using cluster analysis. *J Allergy Clin Immunol*. 2014;133(6):1557–15563 e5.
26. Wu W, Bleecker E, Moore W, et al. Unsupervised phenotyping of Severe Asthma Research Program participants using expanded lung data. *J Allergy Clin Immunol*. 2014;133(5):1280–1288.
27. Kim TB, Jang AS, Kwon HS, et al. Identification of asthma clusters in two independent Korean adult asthma cohorts. *Eur Respir J*. 2013;41(6):1308–1314.
28. Choi S, Hoffman EA, Wenzel SE, et al. Quantitative computed tomographic imaging-based clustering differentiates asthmatic subgroups with distinctive clinical phenotypes. *J Allergy Clin Immunol*. 2017;140(3):690–700. e8.
29. Gupta S, Hartley R, Khan UT, et al. Quantitative computed tomography-derived clusters: redefining airway remodeling in asthmatic patients. *J Allergy Clin Immunol*. 2014;133(3):729–738 e18.
30. Gupta S, Siddiqui S, Haldar P, et al. Quantitative analysis of high-resolution computed tomography scans in severe asthma subphenotypes. *Thorax*. 2010;65(9):775–781.
31. Naidich DP, Webb W, Grenier Richard, Philippe A, Harkin Timothy J, Gefter Warren B. *Imaging of the Airways: Functional and Radiologic Correlations*. Lippincott Williams & Wilkins; 2005:133–134.
32. Sung A, Naidich D, Belinskaya I, et al. The role of chest radiography and computed tomography in the diagnosis and management of asthma. *Curr Opin Pulm Med*. 2007;13(1):31–36.
33. Woodruff PG, van den Berge M, Boucher RC, et al. American thoracic society/national heart, lung, and blood Institute asthma-chronic obstructive pulmonary disease overlap workshop report. *Am J Respir Crit Care Med*. 2017;196(3):375–381.
34. Gibson PG, McDonald VM. Asthma-COPD overlap 2015: now we are six. *Thorax*. 2015;70(7):683–691.
35. Leung JM, Sin DD. Asthma-COPD overlap syndrome: pathogenesis, clinical features, and therapeutic targets. *BMJ*. 2017;358:j3772.
36. Gibson PG, Simpson JL. The overlap syndrome of asthma and COPD: what are its features and how important is it? *Thorax*. 2009;64(8):728–735.
37. Alshabanat A, Zafari Z, Albanyan O, et al. Asthma and COPD overlap syndrome (ACOS): a systematic review and meta analysis. *PLoS One*. 2015;10(9), e0136065.
38. de Marco R, Marcon A, Rossi A, et al. Asthma, COPD and overlap syndrome: a longitudinal study in young European adults. *Eur Respir J*. 2015;46(3):671–679.
39. Montesantos S, Katz I, Venegas J, et al. The effect of disease and respiration on airway shape in patients with moderate persistent asthma. *PLoS One*. 2017;12(7), e0182052.
40. Vasilescu DM, Martinez FJ, Marchetti N, et al. Noninvasive imaging biomarker identifies small airway damage in severe chronic obstructive pulmonary disease. *Am J Respir Crit Care Med*. 2019;200(5):575–581.
41. Hekking PP, Loza MJ, Pavlidis S, et al. Transcriptomic gene signatures associated with persistent airflow limitation in patients with severe asthma. *Eur Respir J*. 2017;50(3).